Optics & Laser Technology 42 (2010) 186–191

Contents lists available at ScienceDirect

Optics & Laser Technology

journal homepage: www.elsevier.com/locate/optlastec

Tight focusing of spirally polarized vortex beams

Jixiong Pu [a,*], Zhiming Zhang [b]

[a] Institute of Optics and Photonics, Huaqiao University, Quanzhou, Fujian 362021, China
[b] Department of Light Current, Mechanical and Electrical Equipments Center, Chengdu Shuangliu International Airport, Chengdu 610200, China

ARTICLE INFO

Article history:
Received 20 April 2009
Received in revised form
26 May 2009
Accepted 12 June 2009
Available online 4 July 2009

Keywords:
Tightly focusing
Spiral polarization
Vortex beams

ABSTRACT

The tight focusing of spirally polarized focused vortex beams is analyzed numerically based on the vectorial Debye theory. The expressions for the electric field and the orbital angular momentum of focused beams are derived. It is shown that the intensity distribution in the focal plane is dependent on the specific spirally polarized state and the coefficient of the spiral polarization function. By presenting the phase contours of the component polarized in the radial direction, it is found that the radii of dislocation lines will increase with the increase of the power of the spirally polarization function. It is reveled that the same orbital angular momentum can be obtained for different spirally polarized state at certain distance along the propagation direction in the focal region. Besides, the orbital angular momentum distributions for different polarized states have fewer crossover points with each other for higher topological charge. The influence of the spirally polarized state on the orbital angular momentum in the focal plane is also studied.

1. Introduction

The orbital angular momentum (OAM) of focused vortex beams has attracted many researchers' interests for years [1–8]. OAM is a contribution to the angular momentum which results from the rotation of phase around the vortex axis [1]. Light beams carrying OAM have generated wide applications in particles' capture, micromachines, spintronics and quantum information etc. [3]. Meanwhile, beam shaping using spatially variant polarization has been of increasing research interest in recent years [9–13]. Bing Hao and James Leger have recently investigated the numerical aperture (NA) invariant focus shaping using spirally polarized beams. They proposed that spirally polarization is another kind of spatially variant polarization [10]. Spiral polarization could be obtained by extending the generalized cylindrical polarized vector beam concept, where the rotated polarization angle is a function of the radius, as shown in Fig. 1. Spiral polarization can be realized in practice by using computer-generated sub-wavelength dielectric gratings [9] or spatial light modulator [11,12]. To the best of our knowledge, there have been no reports of tight focusing of spirally polarized focused vortex beams. Therefore, it is of great interest to revel the influence of variant spirally polarized state on the focused vortex beams.

In this paper, we analyze the tight focusing of vortex beams with spiral polarization. Tight focusing means that the light beam is focused by a high numerical aperture objective and paraxial approximation is not valid anymore. The intensity, phase contours and OAM distribution of the tightly focused spirally polarized vortex beams are investigated in detail using numerical simulation.

2. Theory analysis

The scheme of cylindrical polarization is shown in Fig. 1(a). The rotated angle between the polarization direction and the normal is fixed as ϕ_0. Fig. 1(b) shows the schematic distribution of the spiral polarization. At each point, the polarization can be decomposed into radial and azimuthal basis components. The specific polarization depends on the form of the function $\phi_0(r)$, where r denotes the radius, and the "spiral lines" produce different polarization patterns.

Bessel Gauss (BG) beams of non-zero order have a helical phase structure of $\exp(in\phi)$, therefore they can be treated as vortex beams. The electric field of BG beams propagating along the z-axis has the form

$$E_n(r,\phi,z) = E_0 J_n(\beta r)\exp(-r^2/w_0^2)\exp(in\phi)\exp(-ikz), \quad (1)$$

where $J_n(x)$ is the Bessel function of the first kind of order n, E_0 and w_0 the constants representing amplitude and beam size, respectively. β the parameter corresponding to the Bessel function, n the topological charge, and $k = 2\pi/\lambda$ is the wave number. Since commercial objectives are usually designed to obey the sine condition [14], i.e. $r = f\sin\theta$, where f is the focal length of the objective, the pupil apodization function of the amplitude part of

* Corresponding author.
E-mail address: jixiong@hqu.edu.cn (J. Pu).

0030-3992/$ - see front matter © 2009 Elsevier Ltd. All rights reserved.
doi:10.1016/j.optlastec.2009.06.008

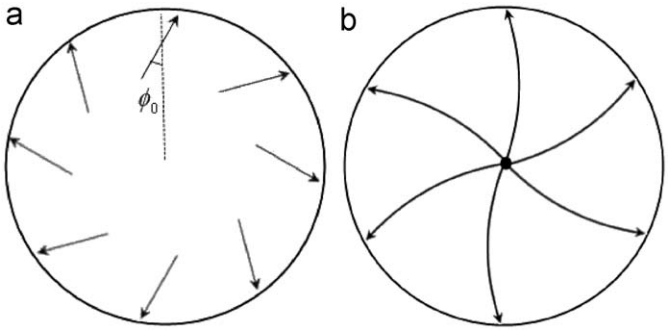

Fig. 1. The scheme of (a) cylindrical polarization and (b) spiral polarization.

BG beams can be written as:

$$P_n(\theta) = E_0 J_n(\beta f \sin\theta)\exp(-f^2\sin^2\theta/w_0^2). \quad (2)$$

And for tightly focused spirally polarized vortex beams, according to the vectorial Debye theory, the electric field distribution in the focal region could be expressed as follows [10,15]:

$$E_r(r,\varphi,z) = \frac{i^n E_0}{2}\exp(in\varphi)\int_0^{\alpha}\cos\phi_0(\theta)\sqrt{\cos\theta}\sin(2\theta)P(\theta) \times \exp[ik(z\cos\theta)]\times[J_{n+1}(kr\sin\theta) - J_{n-1}(kr\sin\theta)]\,d\theta, \quad (3)$$

$$E_\varphi(r,\varphi,z) = i^n E_0\exp(in\varphi)\int_0^{\alpha}\sin\phi_0(\theta)\sqrt{\cos\theta}\sin\theta P(\theta) \times \exp[ik(z\cos\theta)]\times[J_{n+1}(kr\sin\theta) - J_{n-1}(kr\sin\theta)]\,d\theta, \quad (4)$$

$$E_z(r,\varphi,z) = 2i^{n+1}E_0\exp(in\varphi)\int_0^{\alpha}\cos\phi_0(\theta)\sqrt{\cos\theta}\sin^2\theta P(\theta) \times \exp[ik(z\cos\theta)]\times J_n(kr\sin\theta)\,d\theta, \quad (5)$$

where r, φ and z are the cylindrical coordinates of an observation point in the focal region. $\alpha = \sin^{-1}(NA)$ is the maximal angle determined by the NA of the objective, and $P(\theta)$ the pupil apodization function at the objective aperture surface. $\phi_0(\theta)$ is the polarization apodization function corresponds to the specific spiral polarization, which represents the polarized state. In this paper, in order to investigate the characteristic of different spirally polarized states, $\phi_0(\theta)$ is set as $\phi_0(\theta) = A\theta$, $A\theta^2$ and $A\theta^3$, where A is a variable coefficient of the polarization function. On substituting Eq. (2) into Eqs. (3)–(5), the expressions of electric field of spirally polarized BG beams focused by a high NA objective are obtained, therefore the distribution of intensity and phase contours could be analyzed theoretically. The results of substituting Eq. (2) into Eqs. (3)–(5) could be expressed as follows:

$$E_r(r,\varphi,z) = \frac{i^n E_0}{2}\exp(in\varphi)\int_0^{\alpha}\cos\phi_0(\theta)\sqrt{\cos\theta}\sin(2\theta)J_n(\beta f\sin\theta) \times exp(ikz\cos\theta - f^2\sin^2\theta/w_0^2)[J_{n+1}(kr\sin\theta) - J_{n-1}(kr\sin\theta)]\,d\theta, \quad (6)$$

$$E_\varphi(r,\varphi,z) = i^n E_0\exp(in\varphi)\int_0^{\alpha}\sin\phi_0(\theta)\sqrt{\cos\theta}\sin\theta J_n(\beta f\sin\theta) \times \exp(ikz\cos\theta - f^2\sin^2\theta/w_0^2)[J_{n+1}(kr\sin\theta) - J_{n-1}(kr\sin\theta)]\,d\theta, \quad (7)$$

$$E_z(r,\varphi,z) = 2i^{n+1}E_0\exp(in\varphi)\int_0^{\alpha}\cos\phi_0(\theta)\sqrt{\cos\theta}\sin^2\theta J_n(\beta f\sin\theta) \times \exp(ikz\cos\theta - f^2\sin^2\theta/w_0^2)J_n(kr\sin\theta)\,d\theta. \quad (8)$$

The combination of the rotation of field and the longitudinal propagation of vortex beams produces orbital angular momentum [16]. Since the spirally polarized BG beams are passing through a high NA objective, the OAM should be analyzed under the

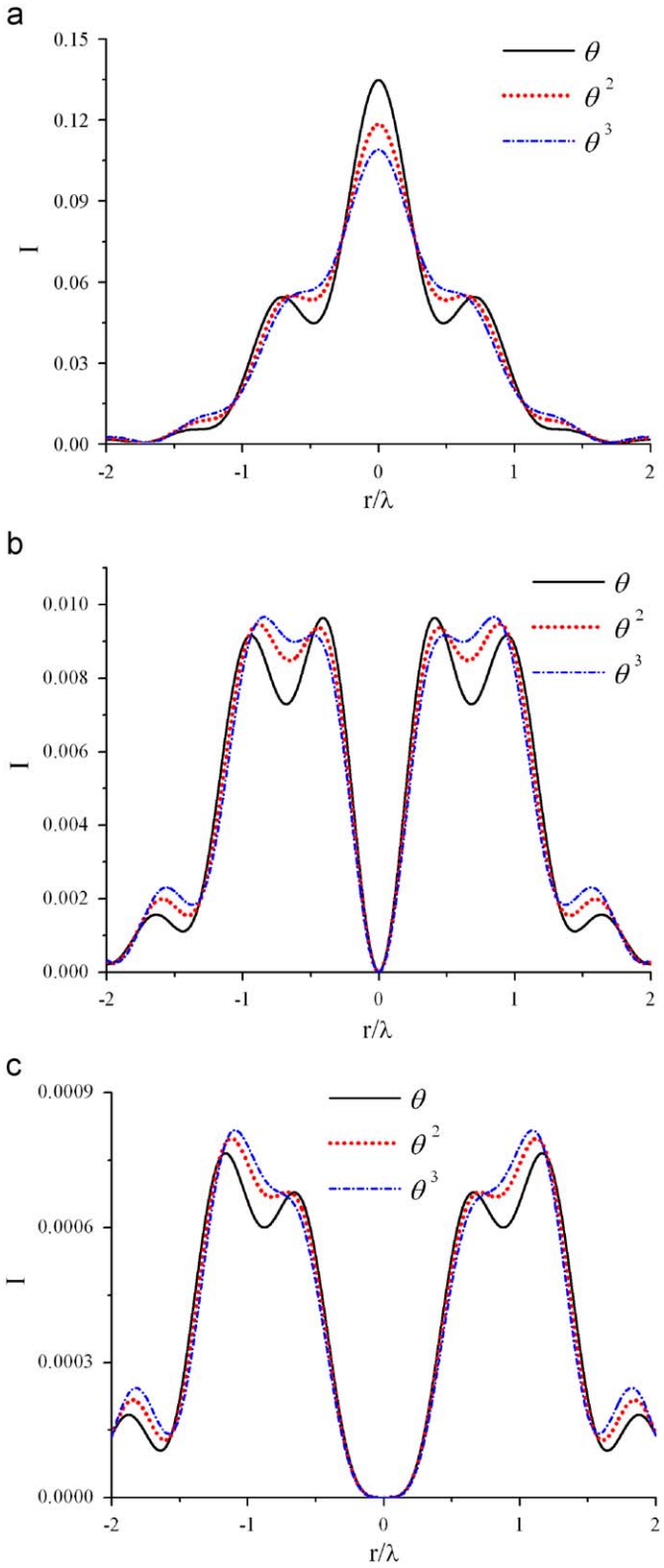

Fig. 2. The intensity distributions as a function of the spirally polarized state in the focal plane at topological charge (a) $n = 1$, (b) $n = 2$ and (c) $n = 3$. The parameters for calculation are: $A = 1$, $NA = 0.9$, $\lambda = 632.8$ nm, d $= 1\lambda$, $\beta = 0{\cdot}25\,\mathrm{mm}^{-1}$, $f = 1$ cm and $w_0 = 2$ cm.

nonparaxial regime. The formula suggested by Ref. [17] for the ratio between the angular momentum and the energy of nonparaxial beams is

$$\frac{J_z}{W}=\frac{(n+\sigma)}{\omega}+\frac{\sigma}{\omega}\frac{\int_0^k d\kappa[|E(\kappa)|^2\kappa/(k^2-\kappa^2)]}{\int_0^k d\kappa[|E(\kappa)|^2(2k^2-\kappa^2)/\kappa(k^2-\kappa^2)]}, \tag{9}$$

where $\kappa=k\sin\theta$ is the special frequency with θ, and ω the frequency of the incident wave. σ the helicity of the light beam which is ±1 for circularly polarized light. Obviously, spin angular momentum is not involved for spirally polarized BG beams, because the polarized direction is fixed and the helicity σ is zero under this condition. Therefore, the second term in Eq. (9) is zero and could be omitted. And only OAM is remained, which is related to the topological charge and the energy of the beam. The OAM density of vortex beams is defined as [16]

$$M_z(r,\phi,z)=-\frac{\varepsilon_0 n}{\omega}|E(r,\phi,z)|^2, \tag{10}$$

where ε_0 is the permittivity of vacuum. Eq. (10) indicates that OAM coincides with the intensity distribution. And the total OAM value L_z is the integral of M_z over the beam cross-section [16]

$$L_z=\int_0^{2\pi}\int_0^{\infty}M_z r\,dr\,d\phi, \tag{11}$$

Therefore, the distribution of OAM of tightly focused spirally polarized BG beams could be investigated by substituting the total intensity into Eq. (11). The total intensity distribution is the summation of Eqs. (6)–(8).

3. Numerical results

The intensity distributions as a function of the spirally polarized state in the focal plane at topological charge $n=1$, 2, 3 are illustrated in Fig. 2. For $n=1$, the central intensity peak will be decreased when the polarized state changes from linear to the

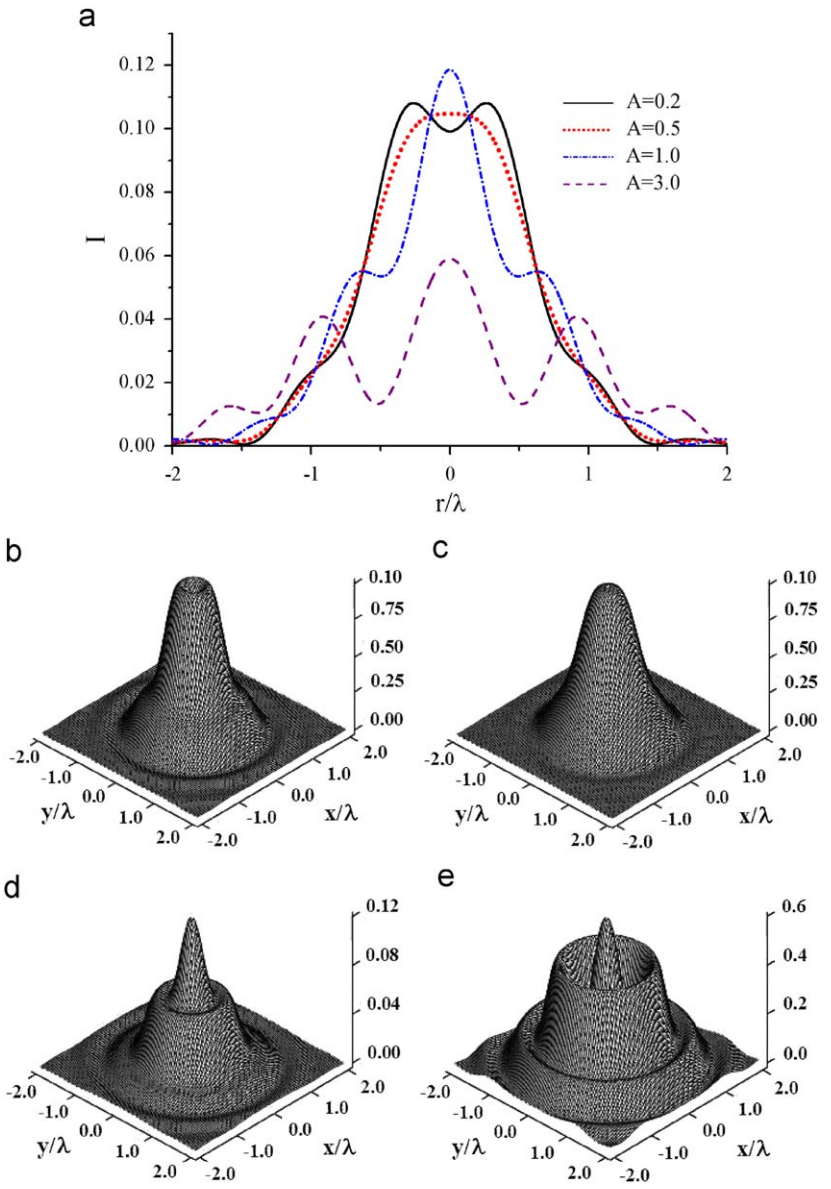

Fig. 3. The dependence of intensity distribution in the focal plane on the coefficient of the spiral polarization function: (a)the total intensity profiles of four different coefficients; (b) the total intensity distribution for $A=0.2$; (c) the total intensity distribution for $A=0.5$; (d) the total intensity distribution for $A=1.0$; (e) the total intensity distribution at $A=3.0$; the parameters for calculation except the variable coefficient A are the same as in Fig. 2(a).

cubic spiral polarization (the polarization apodization function changes from $\phi_0(\theta)=\theta$ to $\phi_0(\theta)=\theta^3$). While, the dark ring between the side shoulders and the central peak will disappear. For $n=2$ and $n=3$, the side intensity peaks' shape also vary with the shift of the spiral polarization. The side shoulders' intensities will increase when the polarized state changes from linear to cubic spiral polarization. Therefore, the intensity distribution in the focal plane is dependent on the spirally polarized state.

Fig. 3 shows the dependence of intensity distribution in the focal plane on the coefficient of the spiral polarization function. The polarization apodization function in this figure is set as $\phi_0(\theta)=A\theta^2$. It is shown that when the coefficient $A=0.2$, the two intensity peaks are located around the origin. Then a flat-top intensity distribution forms at $A=0.5$. For $A=1.0$, it becomes a central intensity peak with two shoulders again. The side lobes become more obvious for $A=3.0$, while the central intensity peak is decreased. So, the coefficient of the spiral polarization function will influence the intensity distribution.

The phase contours of the component polarized in the radial direction are shown in Fig. 4. It is shown that for topological charge $n=1$, there exists one singularity in the center, and the integral around the origin is 2π. And for $n=2$, the integration around the central singularity is 4π. When the spirally polarized state changes from linear to cubic, the phase contours' distribution also changes. Though the variation is not very obvious, one can note that the area of the corner of the phase contours decrease for linear, quadratic and cubic states, respectively. For a more clear comparison, the zoomed in detail of the corner of each phase contours is shown in Fig. 4(g). This phenomenon indicates that the radii of dislocation lines will increase with the increase of the power of the spirally polarization function [7].

The OAM distributions along the propagation direction z-axis are shown in Fig. 5. It should be noted that the curves plotted are normalized to the maximum of the data among the illustrated range of each figure. As shown in Fig. 5(a), when $n=1$ the OAM in the focal plane at $z=0$ is the minimum for all polarized states. The OAM distributions keep on varying along the z-axis. One can see that the relative maximum OAM in different region along the z-axis will be varied among the three polarized states. Furthermore, as shown in the figure, there are more than 10 crossover points which indicating that the same OAM can be obtained for different spirally polarized state at certain distance along the propagation direction. When $n=2$ and $n=3$, however, the OAM in the focal plane no longer takes the minimum as a contrast to $n=1$, as shown in Fig. 5(b) and (c). Besides, there are 9 and 4 crossover points $n=2$ and $n=3$, respectively. Therefore, the OAM distributions for different polarized states have less crossover points with each other for higher topological charge. Therefore, this behavior might be useful for producing the same OAM adopting different spirally polarized states.

The OAM in the focal plane as a function of the spirally polarized state is illustrated in Fig. 6. And the curves for $n=1$ is normalized to the value when the polarized state is quintic. The

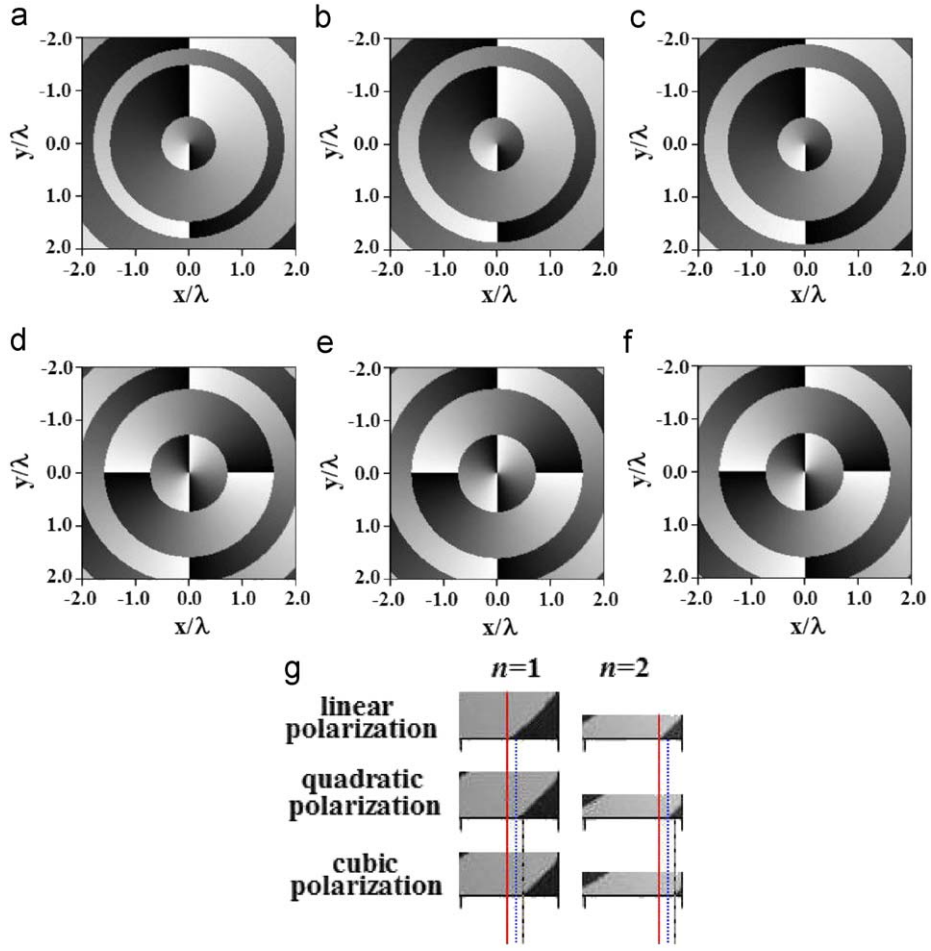

Fig. 4. The phase contours of the component polarized in the radial direction: (a), (b) and (c) for $n=1$; (d), (e) and (f) for $n=2$; (a) and (d) for linear polarized state; (b) and (e) for quadratic polarized state; (c) and (f) for cubic polarized state; (g) zoomed in detail of the corner of each phase contours. The parameters for calculation are the same as in Fig. 2. White (black) shades indicates phase value of $\pi(-\pi)$.

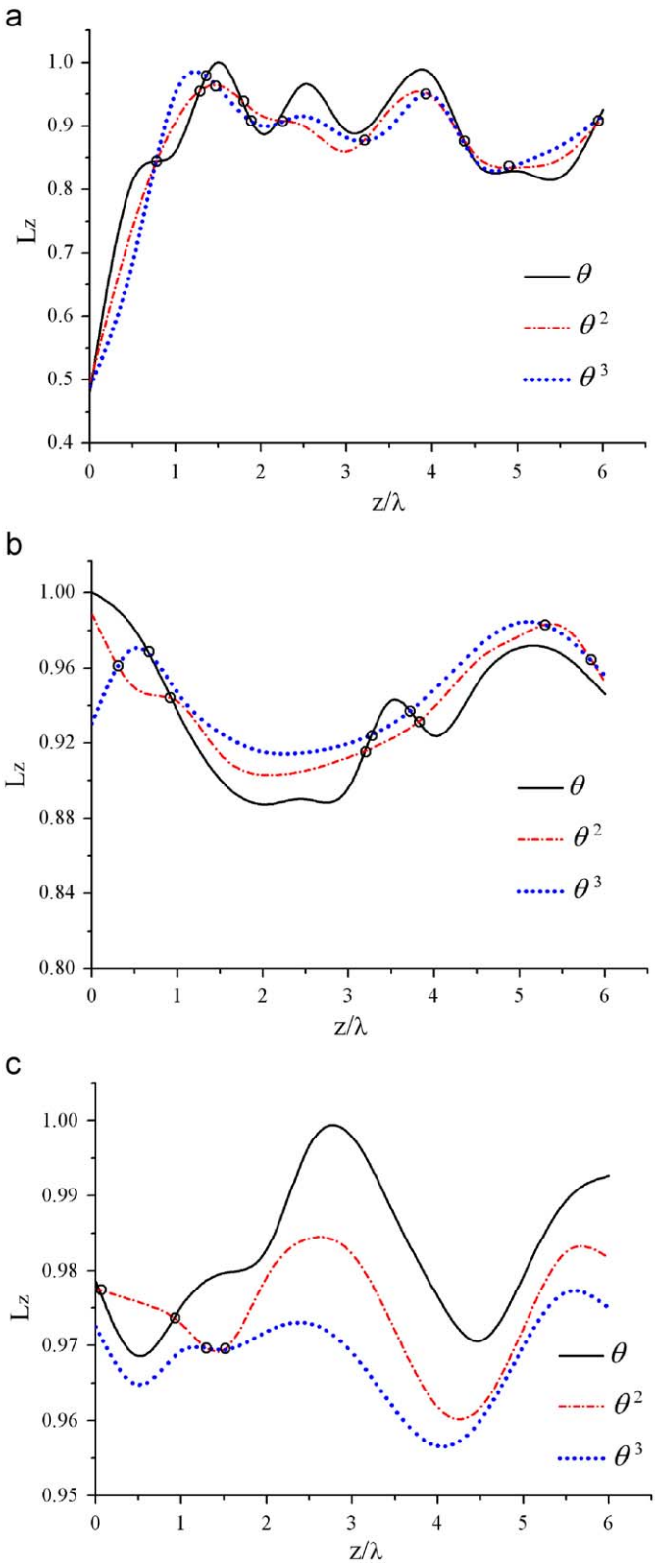

Fig. 5. The OAM distribution along the propagation direction z-axis: (a) $n = 1$; (b) $n = 2$; (c) $n = 3$. The parameters for calculation are the same as in Fig. 2. Crossover points are marked with rings.

curves for $n = 2$ and $n = 3$ are normalized to the value when the spirally polarized state is linear. For $n = 1$, it is shown that the OAM in the focal plane will increase when polarized state changes from linear to quadratic. Then it decreases as the polarization changes to cubic, and finally reaches a maximum for the quintic spirally polarized state. When $n = 2$ the maximum and minimum of the OAM occur at linear and cubic spirally polarized states, respectively. For $n = 3$, the OAM will decrease with the increase of the power of the spirally polarization function consistently. As each curve is normalized to the maximal value, the real magnitudes of OAM for different topological charges cannot be depicted in Fig. 6. However, we can predict that, for the same spirally polarized state, the beams with lower topological charge correspond to higher OAM. Because OAM is determined by the beam's total cross-section intensity and the beams with lower topological charge have higher intensities due to the amplitude distribution [7].

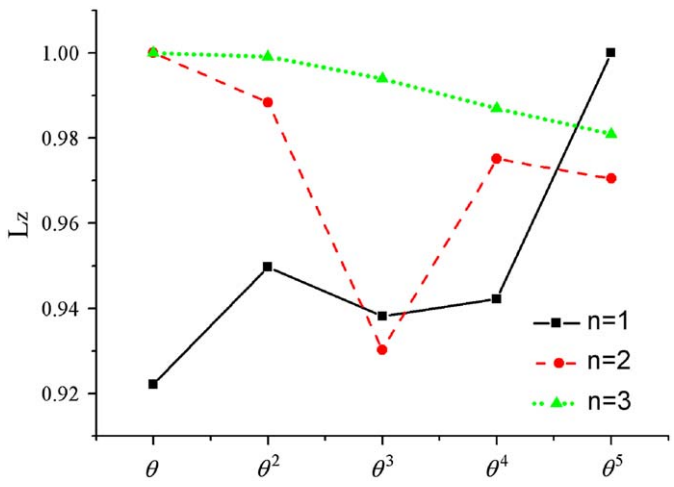

Fig. 6. The OAM in the focal plane as a function of the polarized state. The parameters for calculation are the same as in Fig. 2.

4. Conclusions

We have derived the expressions for the electric field and the OAM of the tightly focused spirally polarized vortex beams. The intensity distribution as a function of the spirally polarized state in the focal plane at different topological charges is studied. It is shown that the intensity distribution in the focal plane is dependent on the specific spirally polarized state and the coefficient of the spiral polarization function. The phase contours of the component polarized in the radial direction are illustrated, finding that the radii of dislocation lines will increase with the increase of the power of the spirally polarization function. It is reveled that the same OAM can be obtained for different polarized state at certain distance along the propagation direction. Besides, the OAM distributions for different spirally polarized states have fewer crossover points with each other for higher topological charge. The OAM in the focal plane as a function of the polarized state is also investigated. Such spatially polarization structure beams may find applications in the circumstances where very small focused spots with flat-tops or hollow beams are desired, and the exact numerical aperture is variable or unknown [10].

Acknowledgements

The research was supported by the Natural Science Foundation of Fujian Province(Grant no. A0810012) and the Key Project of Science and Technology of Fujian Province (Grant no. 2007H0027).

References

[1] Allen L, Beijersbergen MW, Spreeuw RJC, Woerdman JP. Orbital angular momentum of light and the transformation of Laguerre–Gaussian laser modes. Phys Rev A 1992;45(11):8185–9.

[2] Allen L, Padgett MJ. The poynting vector in Laguerre–Gaussian beams and the interpretation of their angular momentum density. Opt Commun 2000; 184(1–4):67–71.

[3] Terriza GM, Torres JP, Torner L. Orbital angular momentum of photons in noncollinear parametric downconversion. Opt Commun 2003;228(1–3): 155–60.

[4] Roux FS. Distribution of angular momentum and vortex morphology in optical beams. Opt Commun 2004;242(1–3):45–55.

[5] Gibson G, Courtial J, Padgett MJ, Vasnetsov M, Pas'ko V, Barnett SM, et al. Free-space information transfer using light beams carrying orbital angular momentum. Opt Express 2004;12(22):5448–56.

[6] Zhao Y, Edgar JS, Jeffries GDM, McGloin D, Chiu DT. Spin-to-orbital angular momentum conversion in a strongly focused optical beam. Phys Rev Lett 2007;99(4):073901.

[7] Zhang Z, Pu J, Wang X. Distribution of phase and orbital angular momentum of tightly focused vortex beams. Opt Eng 2008;47(6):068001.

[8] Nieminen TA, Stilgoe AB, Heckenberg NR, Rubinsztein-Dunlop H. Angular momentum of a strongly focused Gaussian beam. J Opt A—Pure Appl OPt 2008;10(11):115005.

[9] Bomzon Z, Biener G, Kleiner V, Hasman E. Radially and azimuthally polarized beams generated by space-variant dielectric subwavelength gratings. Opt Lett 2002;27(5):285–7.

[10] Hao B, Leger J. Numerical aperture invariant focus shaping using spirally polarized beams. Opt Commun 2008;281(8):1924–8.

[11] Spilman AK, Brown TG. Stress birefringent, space-variant wave plates for vortex illumination. Appl Opt 2007;46(1):61–6.

[12] Novotny L, Beversluis MR, Youngworth KS, Brown TG. Longitudinal field modes probed by single molecules. Phys Rev Lett 2001;86(23):5251–4.

[13] Zhan Q, Leger JR. Focus shaping using cylindrical vector beams. Opt Express 2002;10(7):324–31.

[14] Gu M. Advanced optical imaging theory. Heidelberg: Springer; 2000.

[15] Rao L, Pu J, Chen Z, Yue P. Focus shaping of cylindrically polarized vortex beams by a high numerical-aperture lens. Opt Laser Technol 2009; 41(3):241–6.

[16] Soskin MS, Vasnetsov MV. Progress in Optics. In: Wolf E, editor., Vol. 42. Amsterdam: Elsevier, 2001, p. 219–76.

[17] Barnett SM, Allen L. Orbital angular momentum and nonparaxial light beams. Opt Commun 1994;110(5–6):670–80.